Comparison of different vertically-aligned ZnO nanostructures in excitonic solar cells: Nanorods, Nanocore-shells and Nanotrees.

Irene Gonzalez-Valls and Monica Lira-Cantu*

Centre d'Investigació en Nanociència i Nanotecnologia (CIN2, CSIC), ETSE, Campus UAB, Edifici Q, 2nd Floor, Bellaterra (Barcelona), E-08193, Spain. monica.lira@cin2.es

ABSTRACT

In this work we present the synthesis and photovoltaic application of four different vertically-aligned ZnO nanostructured electrodes: ZnO nanorods prepared by the a) low-temperature hydrothermal method (LT-HM) and the b) autoclave method (A-HM), c) ZnO nanotrees (NTs) and d) ZnO core-shell NRs with an indium sulfide layer as the shell (CS). The electrodes have been applied in Dye sensitized solar cells (DSCs) and Polymer solar cells (PSCs). The photovoltaic properties of each type of nanostructured electrode were optimized separately. Our results show that the optimal power conversion efficiency depends in great extent on NR dimensions (length and diameter) and the final ZnO nanostructure. In this respect, we have observed an increase in power conversion efficiency when the NR nanostructure is modified as follows: ZnO NRs LT-HM < A-HM < NT < CS for Dye semnsitized solar cells. In the case of PSCs the best power conversion efficiency was obtained for the CS sample.

Keywords: ZnO nanorods, surface defects, hydrothermal method, ZnO nanostructures, core-shell nanostructure, Dye-sensitized solar cells, Polymer solar cells, Photoluminescence.

1. INTRODUCTION

The application of vertically-aligned ZnO nanorods (NR) in Excitonic Solar Cells, XSCs, (organic, dye sensitized and hybrid solar cells) has been rising over the last few years due to the excellent optical properties of ZnO.[1] ZnO can be synthesized in a wide variety of nanoforms applying easy, low cost, environmental-friendly and scalable synthesis methodologies.[2, 3] Moreover, the ZnO interface between the donor and acceptor materials can be tune in order to improve power conversion efficiency in polymer solar cells (PSC),[4] or enhance electron injection in Dye sensitized solar cells (DSCs).[5, 6] Up to date, DSCs based on ZnO have already achieved promising power conversion efficiency values of about 6-7%.[7] Nevertheless, the efficiency of DSC applying vertically-aligned ZnO nanorods is still low with power conversion efficiencies not higher than 2.4%.[8] For this reason, many research efforts are currently focused on the synthesis of ZnO nanostructures like hierarchical ZnO nanoplates, nanosheets, disk-like nanostructures and aggregates that can achieve about 5-6% when applied in DSCs.[9] In this work we present the synthesis of ZnO NRs prepared with two different hydrothermal methods, ZnO nanotrees and core-shell structures of ZnO NRs with an indium sulfide layer. The comparison of solar cell performances in DSC and PSC between all the different ZnO nanostructures is described.

2. EXPERIMENTAL

2.1 Materials

All chemicals were commercial and used without further purification. Solvents: Methanol (99.8% Aldrich), ethanol (99.5% Panreac), 2-propanol or also called isopropanol (99.5% Sigma-Aldrich), acetone (99.5% Panreac), chlorobenzene (99.9% Sigma-Aldrich), hydrochloric acid fuming (HCl) (37% Fluka). Chemicals for the ZnO electrode preparation: zinc acetate dehydrate ($Zn(OAc)_2 \cdot 2H_2O$) (99% Riedel-de Haën), potassium hydroxide (KOH) (Na<0.002% Fluka), diethanolamine (DEA) (≥98% Sigma–Aldrich), zinc nitrate hexahydrate ($Zn(NO_3)_2 \cdot 6H_2O$) (98% Sigma–Aldrich),

Next Generation (Nano) Photonic and Cell Technologies for Solar Energy Conversion III, edited by Loucas Tsakalakos, Proc. of SPIE Vol. 8471, 84710X · © 2012 SPIE
CCC code: 0277-786/12/$18 · doi: 10.1117/12.929678

hexamethylenetetramine (HMT) (99% Aldrich), indium (III) chloride (98% Aldrich), sodium thiosulfate (≥98%, Sigma-Aldrich). Fluor-tin oxide (FTO) slides were purchased from Solems (glass thickness= 1.1 mm, FTO thickness=800 Å, R=7-100 Ω). Hydrothermal reactors: Pyrex glass bottle (Sigma-Aldrich) and an autoclave of PTFE (Parr). Materials for Dye-sensitized solar cells: Iodolyte AN-50 (50 mM tri-iodide in acetonitrile), dye $(Bu_4N)_2Ru(debpyH)_2(NCS)$ (Ruthenium 535-bisTBA also known as N719) and hot melt sealing foil (SX1170) were from Solaronix. The Pt source for the counter electrode preparation by electron beam physical vapor deposition was 99.95% from Goodfellow (50 nm thicknes). Materials for polymer solar cells: poly(3,4-ethy-lenedioxythiophene)-poly(styrenesulfonate) (PEDOT:PSS from Agfa, Orgacon EL-P 5010) diluted with 2-propanol (2:1) with a viscosity around 200 mPa·s, polymer Poly(3-hexylthiophene) (P3HT, Sepiolid P200 from BASF), [60]PCBM (99% purchased from Solenne BV), silver flakes (≥99.9%, Aldrich). All the aqueous solutions were prepared using double distilled and ion-exchange water.

2.2 Preparation and characterization of ZnO electrodes.

FTO (Fluor-indium-tin oxide)-coated glass were used to prepare the ZnO electrodes. First, a ZnO sol-gel solution, prepared from zinc acetate and diethanol amine (DEA)[10] was deposited by spin-coating at 1500 rpm on top of clean FTO slides. Then the substrates were sintered at 450ºC/2h. ZnO nanoparticles (NPs) synthesized by Pacholski *et. al.* method[11] were spin coated 3 times at 1000 rpm on the ZnO buffer layer prepared before, between layers the slides were dried at 150ºC for 10 min. The growth of ZnO nanorods (NRs) was carried out using two different hydrothermal growth methods, a low-temperature hydrothermal method (LT-HM) and a modified method with an autoclave reactor (A-HM). Both hydrothermal syntheses use an equimolar aqueous solution of 25 mM zinc nitrate hexahydrate and HMT, growth times were between 6h and 28h. The aqueous solutions were changed every 6h. For the LT-HM method, a Pyrex glass bottle was used as reactor (96ºC and at atmospheric pressure),[12] for the A-HM method an stainless steel autoclave was used. Finally, the samples were rinsed with deionized water, dried in air and then sintered at 450°C for 30 min. Core-shell structures were also prepare using the ZnO NRs electrodes prepared by LT-HM and A-HM. The shell layer of indium sulfide was deposited by SILAR technique. The ZnO NR electrodes were immersed first in a 0.1 M $InCl_3$ aqueous solution then in a 0.03 M of Na_2S (the pH of Na_2S solution was controlled between 7-8 adjusted with a 0.2 M solution of HCl) and finally in distilled H_2O for 3, 5 and 10 cycles. After the substrates were dried with N_2 they were annealed at 200ºC/30 min.[13] Characterization of the ZnO electrodes was carried out in a scanning electron microscopy (SEM, HITACHI-S-570), transmission electron microscopy (TEM, JEOL 2011 operated at 200 kV). X-ray powder diffraction analyses between 5 and 120 degrees were carried out in a XRD, RIGAKU Rotaflex RU200 B instrument, using $CuK\alpha_1$ radiation. Room-temperature photoluminescence (PL) measurements were made with a Kimmon IK Series He-Cd CW laser (325 nm and 40 mW). Fluorescence was dispersed through an Oriel Corner Stone 1/8 74000 monochromator, detected with a Hamamatsu R928 photomultiplier, and amplified through a Stanford Research Systems SR830 DSP Lock-in amplifier.

2.3 Solar cells fabrication and characterization

Dye-sensitized solar cells (DSCs) were prepared: FTO/ZnONRs were first sensitized in a 0.5 mmol/L solution of N719 dye in ethanol at different times. Platinized FTO counter electrode was then bounded thermally together with the ZnO electrode using a hot melt sealing foil and a liquid electrolyte was used to fill the internal space between electrodes. For Polymer solar cells the ZnO electrodes were annealed first at 140°C for 5 minutes and then the organic solution P3HT:PCBM was spin-coated on top. The blend P3HT:PCBM concentration was 40:40 mg/mL in chlorobenzene. Different blend deposition speeds were used: 1500 rpm, 800 rpm, 400 rpm and 2 times 400 rpm (400 rpm + 400 rpm), the drops of the blend solution were first added and then the spin-coater was started. The following step was the PEDOT:PSS deposition at 1000 rpm and after an annealing process at 140°C for 5 minutes.[14] At the end the silver counter-electrode was deposited by vacuum evaporation at a $\sim 10^{-6}$ Torr pressure. The extra active area from outside the silver deposited counter-electrode was scratched and cleaned with chlorobenzene and 2-propanol to remove the organic components. Active areas were around ~ 0.25-0.3 cm^2 (after scratch), measured carefully for each cell. The solar simulation was carried out with a Steuernagel Solarkonstant KHS1200. Light intensity was adjusted at 1000W/m^2 with a bolometric Zipp & Konen CM-4 pyranometer. Calibration of the sun simulator was made by several means applying a calibrated S1227-1010BQ photodiode from Hamamatsu and a minispectrophotometer from Ava-Spec 4200. The AM1.5G reference spectrum was according to ASTM G173 standard. IV-curves were measured using a Keithley 2601 multimeter connected to a computer and software. IPCE analyses were carried out with a QE/IPCE measurement System from Oriel at 10 nm intervals between 300 and 700 nm. The results were not corrected for intensity losses due to light absorption and reflection by the glass support.

3. RESULTS AND DISCUSSION

3.1 Preparation of ZnO nanostructured electrodes

Four different electrodes made of vertically-aligned ZnO nanostructures were prepared and applied in dye sensitized solar cells (DSCs) and polymer solar cells (PSCs): two types of bare ZnO nanorods (NRs), nanotrees (NT) and Core-shell Nanorods (CS). The first two nanostructures are bare ZnO nanorods (NR) obtained by the standard low-temperature hydrothermal methods (LT-HM), also known as chemical bath deposition. All the synthesis conditions were optimized as described before.[15] The same synthesis procedure was followed in order to obtain the second type of bare ZnO NRs, in this case, however, the ZnO NRs were obtained in a pressurized autoclave (A-HM). For comparison purposes of these two types of ZnO NRs, all synthesis conditions were kept the same and special emphasis was made to synthesize the NRs at the same periods of growth time. Thus, the main difference between the ZnO NRs obtained by the LT-HM and the A-HM is the reaction container that, in the first case is a glass reactor and in the second case a stainless steel autoclave reactor.[16] Results show that, for the same reaction time, the ZnO NRs obtained by the A-HM method are 1/5 times shorter in length than the ZnO electrodes obtained by the LT-HM, an indication of the great effect of the pressurized autoclave on NR dimensions. The latter is clearly observed on the SEM images of Figure 1. Figure 1 a-b correspond to the ZnO NR grown by the LT-HM and Figure 1c-d to NRs grown by the A-HM, grown for 6 h and 22 h respectively. Besides the clear difference in NR length, we can also observe a needle-tip morphology, and a more homogeneous distribution of NR diameter for the NR grown by the A-HM. X-Ray diffraction analyses (Figure 2a) together with TEM analyses (Figure 3a-f), revealed that the ZnO electrodes prepared by the LT-HM and A-HM methods show an hexagonal wurtzite crystalline structure. Important differences on surface defects were find by photoluminescence (PL) and time resolved photoluminescence (TRPL).[16] Less surface defects were find on the ZnO NR obtained by the A-HM [16]. Lower surface defects imply less electron traps on the ZnO surface and thus less electron recombination is expected. Time-resolved photoluminescence (TRPL) technique also agreed with PL results: larger electron lifetime was observed for the ZnO NRs obtained by the A-HM electrodes (between 50 and 140 ps) compared to LT-HM electrodes (20-30 ps).[16]

In order to obtain our third nanostructure, this is, the vertically-aligned ZnO nanotrees (NT), the reaction time of the A-HM was increased up to 28 h. At this reaction time the NRs no longer grow vertically, but an open structure on the top of the NR is formed (See Figure 1e). The result is a vertically arrangement of nanotrees-like electrode characterized by nanorod shape on the bottom and an open structure on the top. The NTs can be seen as a nanostructure that can combine the good electron transport properties of NRs with the higher surface area of the top open structure. Thus an optimized nanostructure for light harvesting is obtained.

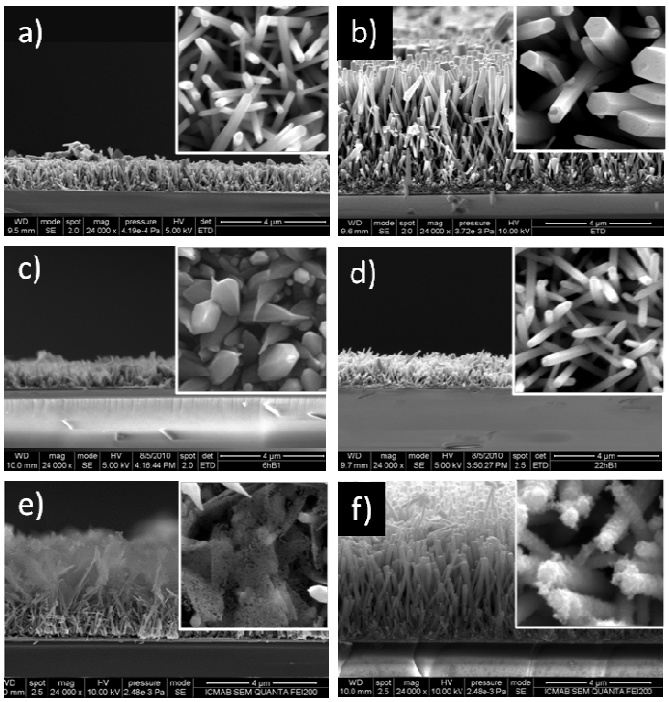

Figure 1. Cross-section and top SEM images of the different ZnO nanostructures: Bare ZnO nanorods grown by the LT-HM at 6h (a) and 22h (b) and by the A-HM grown at 6h (c) and 22h (d). ZnO Nanotrees grown at 28h (e) and core-shell NRs grown for 12h and 5 cycles of SILAR deposition technique (f). The scale of the SEM top images is 1 µm for each square side.

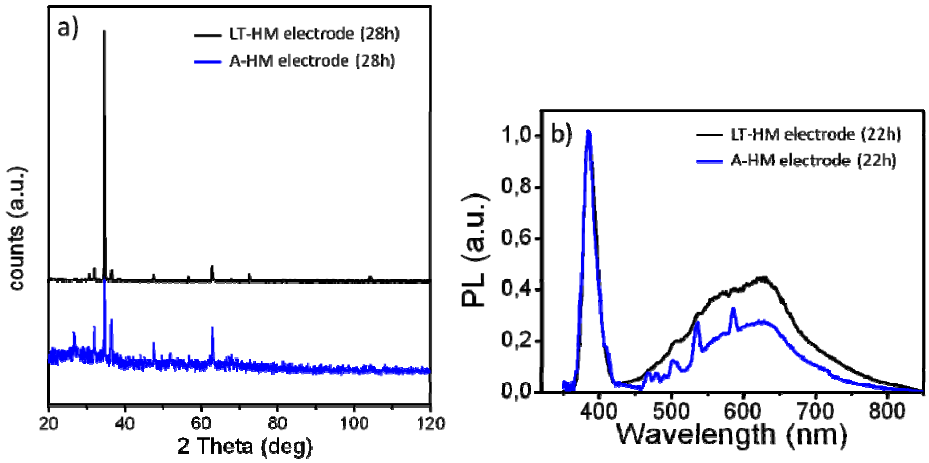

Figure 2. a) X-rays diffraction analysis (XRD) and b) photoluminescence (PL) studies of the ZnO NRs obtained by the LT-HM and the A-HM method grown at different reaction time.

The forth and last nanostructure is the In_xS_y core-shell ZnO NR (CS). This nanostructure presents a core of ZnO NR and a shell of indium sulfide semiconductor in the form of nanoparticles. The indium sulfide (In_2S_3) semiconductor was chosen as shell layer for their bandgap (2.0-2.3 eV) since it could enhance the injection of photogenerated electrons into ZnO.[17] Among all the possible deposition techniques for the outer shell layer, the SILAR method was selected for being

an easy and low-cost fabrication method. The technique consists of the immersion of the ZnO NRs in an aqueous solution of $InCl_3$ followed by a second immersion in a solution of Na_2S. The bare ZnO NRs were obtained by the LT-HM and A-HM methodology described above. Thus, the electrodes with the corresponding core-shell nanostructures are labeled as CS_{LT} and CS_A respectively. The deposition conditions for the In_xS_y have been carefully optimized as reported elsewhere.[18] Figure 1f shows a CS_{LT} electrode, where the ZnO NR was grown for 12h and the indium sulfide shell was made applying 5 SILAR cycles. The top view of the SEM image in Figure 3g, reveals that the ZnO NR structure is maintained after the SILAR method is applied and a well-distributed nanoparticles of the In_xS_y are deposited on the surface. TEM analyses (See Figure 3g-h) indicate that the ZnO NRs from the core present the wurzite crystalline structure, and that the In_xS_y shell layer is not crystalline.

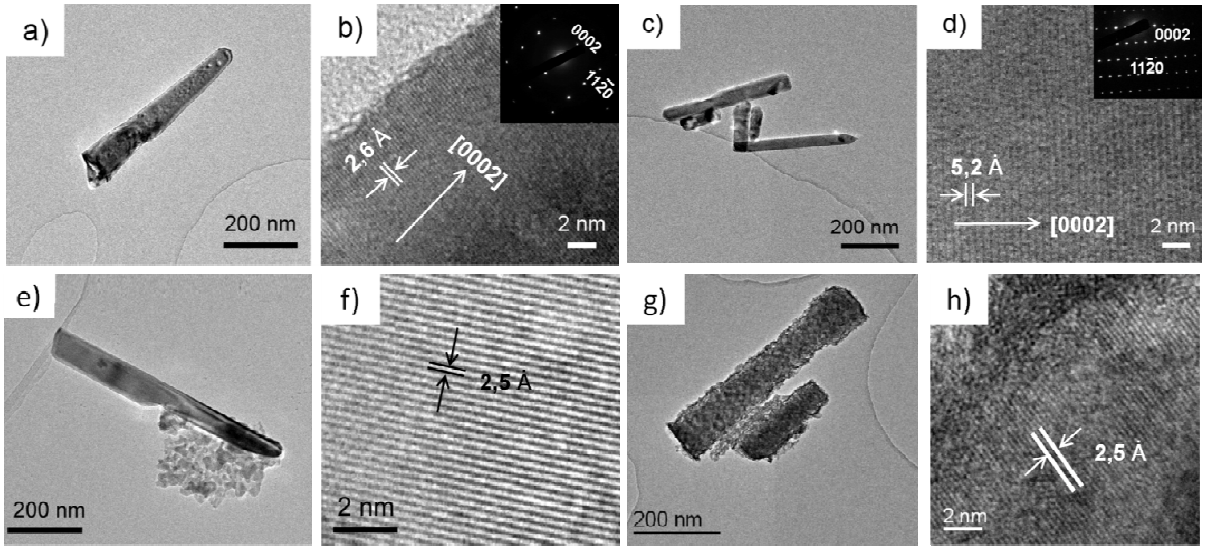

Figure 3. High resolution TEM images and SAED patterns representative of the different ZnO nanostructures: The bare ZnO NRs obtained at 22h by the LT-HM (a-b) and the A-HM (c-d). The NTs (e-f), and the CS_A obtained from ZnO NR grown for 12h and 5 SILAR cycles (h-g).

3.2 Solar cells fabrication

The different ZnO nanostructured electrodes were applied in Dye-sensitized solar cells (DSC) and Polymer solar cells (PSC). To prepare DSCs, the electrodes were immersed in a solution of N719 dye ($(Bu_4N)_2Ru(debpyH)_2(NCS)$), also known as Ruthenium 535-bisTBA. Then the platinum counter-electrode was bounded with a sealing foil and the liquid electrolyte introduced. The dye-loading time was optimized for each ZnO electrode. In general, longer NRs require longer immersion times. The optimal dye loading time were observed when the decrease on solar cell performance is observed due to the formation of $[Zn\text{-}dye]^{2+}$ aggregates.[6] The best power conversion efficiencies obtained in DSC for each electrode type, are presented in Table 1 and the corresponding IV-curves are shown in Figure 4. Longer ZnO NRs presented higher performances for both hydrothermal synthesis methods. An efficiency increase of 25% was achieved for A-HM electrodes with shorter NRs compared with LT-HM electrodes and a 60% increase when ZnO nanotrees were applied in DSCs. The core-shell nanostructures presented the highest performance with a 2.32% power conversion efficiency. All these values are clearly dependent on NR length.

An inverted Polymer solar cells were prepared applying the ZnO electrodes as the electron extracting layer, applying P3HT and PCBM as active materials. The inverted configuration of these cells was FTO/ZnO NRs/ P3HT:PCBM/PEDOT:PSS/Ag. The active organic blend of P3HT:PCBM was deposited on top of the ZnO nanostructured electrodes by spin-coating. Then the PEDOT:PSS layer was also deposited by spin-coating and the Ag counter-electrode evaporated under vacuum. Our results show that shorter ZnO NRs achieved higher performance. The latter is attributed to infiltration issues of the active layer into long ZnO NRs. The latter also explains the low efficiency of ZnO nanotrees obtained. The top structure of the nanotrees avoided the organic blend solution penetration into the

ZnO nanostructure. An improvement on power conversion efficiency was observed for the core-shell electrodes with values around 2% (See Figure 4 and Table 1).[14]

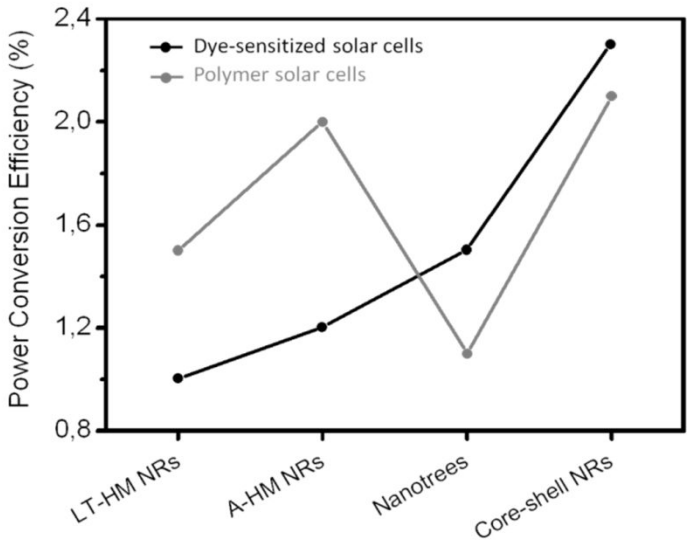

Figure 4. Power conversion efficiency for the different vertically-aligned ZnO nanostructures applied in DSCs and PSCs: Nanorods (NRs) synthesized by the LT-HM and the A-HM methods, nanotrees (NT) and core-shell nanorods (CS).

Table 1. Best performance obtained for DSC and PSC with ZnO nanostructured electrodes. Photovoltaic performance measured at 1.5 AM at 1000 $W \cdot m^{-2}$.

Type of Solar Cell	Growth Time	Synthesis Method	ZnO nanostructure	Length (μm)	V_{oc} (V)	J_{sc} (mA/cm^2)	FF (%)	Efficiency (%)
Dye-sensitized SC	22h	LT-HM	Nanorods (LT_HM)	5.0	0.603	3.72	45	1.01
	22h	A-HM	Nanorods (A-HM)	1.0	0.705	3.50	50	1.24
	28h	A-HM	Nanotrees (NT)	3.0	0.656	6.15	38	1.53
	12 h	SILAR	Core-shell NRs (CS)	3.0	0.702	5.46	60	2.32
Polymer SC	6h	LT-HM	Nanorods (LT_HM)	1.6	0.493	9.65	32	1.51
	6h	A-HM	Nanorods (A-HM)	0.4	0.492	11.63	35	1.96
	28h	A-HM	Nanotrees (NT)	3.0	0.459	8.25	28	1.07
	6 h	SILAR	Core-shell NRs (CS)	0.4	0.548	10,37	31	2,14

Figure 5 shows the IV-curves and IPCE analyses of DSC and PSC cells with all the different ZnO nanostructured electrodes. For the application of the ZnO nanostructures in DSCs (see Figure 5a) an improvement of the open circuit voltage (V_{oc}) was observed when the ZnO electrodes were obtained by the A-HM in comparison with the LT-HM electrode. The response has been attributed to the different amount of the ZnO surface defects: larger amount of surface defects reduces V_{oc} and FF. The application of electrodes made by ZnO nanotrees induce an increase in the current density (J_{sc}), attributed to the larger amount of dye adsorbed on the ZnO nanostructure and the increase in the light harvesting properties of the electrodes.

Finally, the core-shell nanostructure shows an increase of J_{sc} in comparison with the bare ZnO NRs. This effect is attributed to the enhanced porous surface that can absorb higher amount of dye which translates to a better fill factor (FF). The FF improves due to the presence of the indium sulfide shell that helps the charge transfer between the dye and ZnO avoiding charge recombination. The latter is corroborated in figure 5b. The IPCE peak related to the dye (around 550 nm) was higher for the core-shell cell which implies that the dye harvests more light. In the case of PSCs (Figure 5c) the A-HM NRs showed the highest J_{sc} value and the core-shell electrode the highest V_{oc} value. The FFs in these cells were very low due to the organic solution infiltration problems mentioned before. IPCE graphs for PSCs (Figure 5d) presented a big peak for the P3HT and PCBM performance, however, the ZnO peak (around 380 nm) was very low. A surprising low IPCE spectrum for the core-shell cell was observed. Nevertheless, the peak for ZnO on core-shell electrode was the highest and this could explain the higher power conversion efficiency obtained for this electrode.

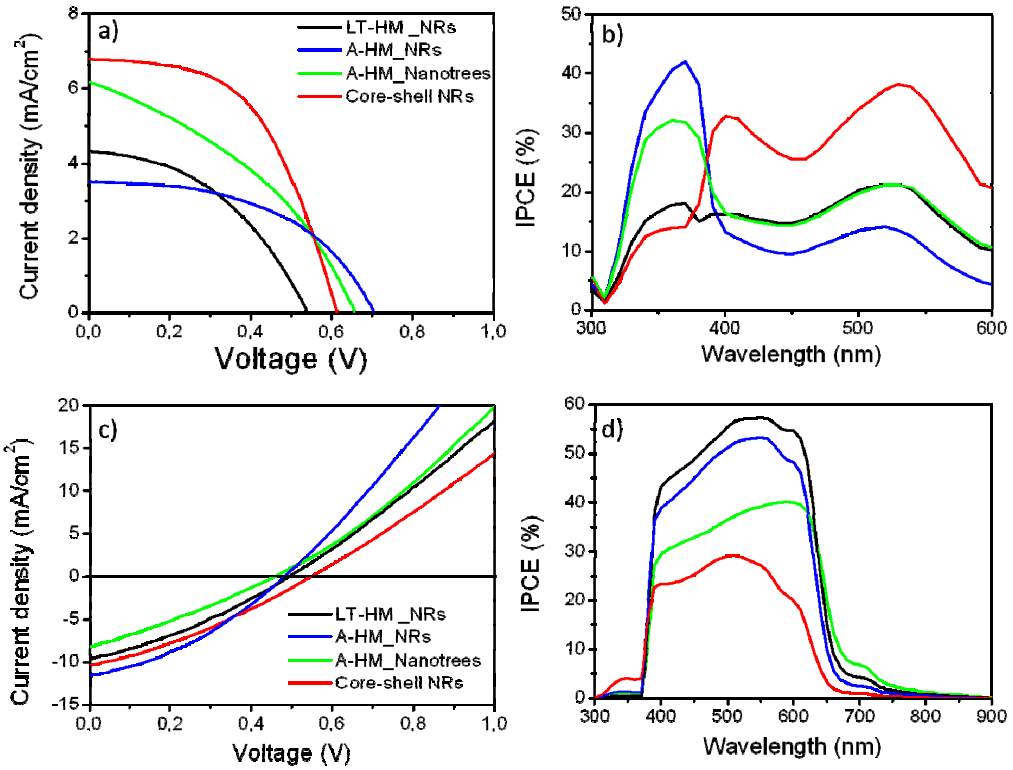

Figure 5. Photovoltaic properties (IV-curve and IPCE) for the 4 types of vertically-aligned ZnO nanostructured electrodes applied in DSC (a-b) and PSC (c-d).

4. CONCLUSIONS

We have synthesized four different ZnO nanostructured electrodes: two bare ZnO NRs obtained by the low temperature hydrothermal mehtod (LT-HM) and the autoclave method (A-HM), nanotrees (NT) and the In_xS_y core-shell ZnO Nanorods (CS). All these electrodes were characterized by SEM, TEM microscopy, x-ray diffraction analyses (XRD) and photoluminescence spectra (PL). The different ZnO nanostructures were applied in dye-sensitized solar cells (DSC) and polymer solar cells (PSC). A comparison of the best results obtained for each ZnO nanostructured electrode in the solar cell devices is presented. Comparison between ZnO NRs obtained by the LT-HM and the A-HM revealed best power conversion efficiencies for the A-HM electrodes due to the reduced amount of surface traps. Longer ZnO NRs presented better performances in DSCs, however lower performances in PSCs. The latter was caused by a poor organic P3HT:PCBM blend infiltration into the long ZnO NRs. The ZnO nanotrees had good performances in DSCs but low in PSC due also to the worse infiltration problems observed on this nanostructure. Higher power conversion efficiencies were observed when the core-shell electrode was used in DSC (2.32%) and PSC (2.14%).

Acknowledgements

To the Spanish Ministry of Science and Innovation, MICINN for the projects ENE2008-04373 and the FPI scholarship EEBB-2011-44415 awarded to I.G-V. To the Consolider NANOSELECT project (CSD2007-00041) and to the Xarxa de Referència en Materials Avançats per a l'Energia, XaRMAE (Reference Center for Advanced Materials for Energy) of the Catalonia Government.

REFERENCES

[1] I. Gonzalez-Valls, and M. Lira-Cantu, "Vertically-aligned nanostructures of ZnO for excitonic solar cells: a review," Energy & Environmental Science, 2(1), 19-34 (2009).
[2] Z. L. Wang, "Nanostructures of zinc oxide," Materials Today, 7(6), 26-33 (2004).
[3] Q. F. Zhang, C. S. Dandeneau, X. Y. Zhou *et al.*, "ZnO Nanostructures for Dye-Sensitized Solar Cells," Advanced Materials, 21(41), 4087-4108 (2009).
[4] M. Lira-Cantu, F. C. Krebs, P. Gomez-Romero *et al.*, Mater. Res. Soc. Symp. Proc., 1007-S14-04 (2007).
[5] M. Law, L. E. Greene, and P. D. Yang, "Nanowire solar cells," Abstracts of Papers of the American Chemical Society, 230, U2048-U2049 (2005).
[6] I. Gonzalez-Valls, and M. Lira-Cantu, "Dye sensitized solar cells based on vertically-aligned ZnO nanorods: effect of UV light on power conversion efficiency and lifetime," Energy & Environmental Science, 3(6), 789-795 (2010).
[7] K. Park, Q. F. Zhang, B. B. Garcia *et al.*, "Effect of an Ultrathin TiO2 Layer Coated on Submicrometer-Sized ZnO Nanocrystallite Aggregates by Atomic Layer Deposition on the Performance of Dye-Sensitized Solar Cells," Advanced Materials, 22(21), 2329-2332 (2010).
[8] M. Guo, P. Diao, X. D. Wang *et al.*, "The effect of hydrothermal growth temperature on preparation and photoelectrochemical performance of ZnO nanorod array films," Journal of Solid State Chemistry, 178(10), 3210-3215 (2005).
[9] T. Yoshida, J. B. Zhang, D. Komatsu *et al.*, "Electrodeposition of Inorganic/Organic Hybrid Thin Films," Advanced Functional Materials, 19(1), 17-43 (2009).
[10] M. Lira-Cantu, and F. C. Krebs, "Hybrid solar cells based on MEH-PPV and thin film semiconductor oxides (TiO2, Nb2O5, ZnO, CeO(2)and CeO2-TiO2): Performance improvement during long-time irradiation," Solar Energy Materials and Solar Cells, 90(14), 2076-2086 (2006).
[11] C. Pacholski, A. Kornowski, and H. Weller, "Self-assembly of ZnO: From nanodots, to nanorods," Angewandte Chemie-International Edition, 41(7), 1188-1191 (2002).
[12] L. Vayssieres, "Growth of arrayed nanorods and nanowires of ZnO from aqueous solutions," Advanced Materials, 15(5), 464-466 (2003).
[13] C. Herzog, A. Belaidi, A. Ogacho *et al.*, "Inorganic solid state solar cell with ultra-thin nanocomposite absorber based on nanoporous TiO(2) and In(2)S(3)," Energy & Environmental Science, 2(9), 962-964 (2009).
[14] I. Gonzalez-Valls, D. Angmo, S. A. Gevorgyan *et al.*, "Study of ZnO NRs surface defects and dimensions for highly efficient Polymer Solar Cells," Submitted, (2012).
[15] I. Gonzalez-Valls, Y. Yu, B. Ballesteros *et al.*, "Synthesis conditions, light intensity and temperature effect on the performance of ZnO nanorods-based Dye sensitized solar cells," Journal of Power Sources, 196, 6609–6621 (2011).
[16] I. Gonzalez-Valls, J. S. Reparaz, F. Güell *et al.*, "Low temperature growth of vertically-aligned ZnO nanorods for dye sensitized solar cells: unravelling their low power conversion efficiency," Submitted (2012).
[17] T. Dittrich, D. Kieven, M. Rusu *et al.*, "Current-voltage characteristics and transport mechanism of solar cells based on ZnO nanorods/In_2S_3/CuSCN," Applied Physics Letters, 93(5), (2008).
[18] I. Gonzalez-Valls and M. Lira-Cantu. *In preparation.*